RADIOGRAPHIC EVALUATION OF RADIAL FLEXION OSTEOTOMY EFFECT ON STATIC SCAPHOLUNATE INSTABILITY: A PRELIMINARY CADAVERIC STUDY.

Short running page heading: RADIAL FLEXION OSTEOTOMY FOR SCAPHOLUNATE INSTABILITY

Rodrigo Cañadillas-Rueda, MD[1], Claudia Sánchez-Agesta, MD[2], Mª Ángeles Villazán-Cervantes, MD[2], Olga Roda, PhD[3]; Indalecio Sánchez-Montesinos García, PhD[3]; Pedro Hernández-Cortés, PhD [2, 4, 5].

1. Orthopedic Surgery Department. University Hospital of Jaen, Spain.
2. Surgery Department, School of Medicine, Granada University, Spain.
3. Department of Human Anatomy, School of Medicine, Granada University, Spain.
4. Upper Limb Surgery Unit. Orthopedic Surgery Department. University Hospital of Granada, Spain.
5. Biosanitary Research Institute of Granada.

Corresponding Author: Olga Roda Murillo.
Anatomy Department. School of Medicine of Granada

Avenida de la Investigación, 11. 18016 Granada, Spain.
orroda@ugr.es

Conflict of Interest: No. Funding: No. No Disclaimer.

All data collected and statistical analyzes performed are available for review.

All illustrations are originals and must be published in colour.

ABSTRACT

Introduction: The optimal treatment of chronic scapholunate instability has yet to be established. Scapholunate ligament grafts are still far from being the ideal solution.

We conducted an experimental study to evaluate whether flexion-opening wedge osteotomy of the distal radius improves misalignment and avoids rotatory subluxation of the scaphoid in a cadaveric model of static scapholunate dissociative instability.

Materials and Methods: Radiographic studies were performed on 15 cryopreserved specimens after recreating a model of scapholunate instability by division of the scapholunate interosseous ligament (SLIL) and secondary stabilizers, taking radiographs at baseline, after the instability model, and after distal radius osteotomy. Static and dynamic (under controlled tendon traction) anteroposterior and lateral views were obtained to measure the length (in mm) of the carpal scaphoid and scapholunate interval, scapholunate angle, radio-lunate angle, and palmar tilt of the distal joint surface of the radius and to measure the dorsal scaphoid translation by the concentric circles method. The Wilcoxon test was used for statistical comparisons.

Results: The scapholunate interval was significantly decreased after osteotomy in all static anteroposterior views and in all lateral views under tendon traction. Dorsal scaphoid translation was significantly reduced in static lateral view in extension and in dynamic lateral view under 5-pound flexor carpi radialis tendon tension controlled by a digital dynamometer.

Conclusion: Flexion-addition osteotomy of the distal radius appears to improve carpal alignment parameters in a cadaveric model of static scapholunate instability, achieving similar values to those obtained before instability

Key Words: Scapholunate instability; distal radius osteotomy; wrist biomechanics; radiographic assessment; carpal alignment.

INTRODUCTION

Scapholunate instability is a frequent cause of wrist pain [1] and can often develop into wrist arthrosis if not treated [2]. The scapholunate intrinsic ligament (SLIL) is the primary stabilizer of the scapholunate joint, while a major role in secondary stabilization is played by various adjacent carpal ligaments such as the dorsal radiocarpal and dorsal intercarpal, scaphotrapeziotrapezoid, and long radioscaphocapitate ligaments [3-6]. Both SLIL lesion and incompetent secondary stabilizers are necessary for static changes in scaphoid and lunate positions [6-8]. Therefore, scapholunate instability is not a single lesion but rather a spectrum of lesions that can affect different structures and has conventionally been classified as predynamic, dynamic, or static according to radiographic behavior [9], arthroscopic examination findings [10-12], and pathological criteria, including ligament remnant tissue, reducibility, or associated chondral damage [13].

Increased instability can lead to a gradual positioning of the scaphoid in palmar flexion and pronation and to its movement in dorsal and radial directions [14,15]. This results in an incongruence of the radius-scaphoid joint, whose contact area is reduced to an elliptic shape and relocated on the dorsal ridge of the radius [2,16]. The scaphoid could be described as acting like a skateboarder, hoisting itself onto the “skate ramp” represented by the dorsal lip of the radius. This finding is consistent with the scaphoid being the first joint affected in arthrosis by scapholunate advanced collapse (SLAC wrist) [17].

Numerous surgical treatments have been described for each stage of scapholunate instability from acute SLIL lesion to SLAC wrist. However, the

optimal surgical procedure has yet to be established [18,19] for chronic scapholunate instability with no degenerative changes but irreparable SLIL (Stage 4) [13].

Treatments are often aimed at the repair or substitution of SLIL using soft tissue reconstruction procedures. Capsulodesis and tenodesis remain the most frequent surgical approaches to reconstruct SLIL instability [20]. However, capsulodesis is associated with postoperative lack of wrist flexion, minimal improvement in radiographic parameters, and failure to preserve radiographic improvement over the long term [21,22]. Likewise, the association of tenodesis with progressive deterioration of carpal radiographic alignment means that 30% of patients require revision surgery, and the development of degenerative joint changes has been observed in up to 63% of patients with an apparently satisfactory surgical outcome [23,24].

We hypothesized that outcomes could be improved by a bone procedure that preserves the joint without soft tissue reconstruction. Accordingly, an experimental study was developed in a cadaveric model of static scapholunate dissociative instability to evaluate whether open wedge distal radius flexion-addition osteotomy improves misalignment and avoids rotatory scaphoid subluxation.

MATERIAL AND METHODS

In this experimental study, the effect of distal radius flexion osteotomy on carpal alignment was assessed by static and dynamic radiographic methods in a cadaveric model of scapholunate dissociation/instability. Fifteen cryopreserved

specimens were used from eight individuals (four males and four females) aged between 58 and 78 years who had donated their bodies to science. The cadaveric upper extremities had no physical examination findings of interest or radiographic evidence of injury, instability, or degenerative changes. Eight right wrists and seven left wrists were dissected and treated after thawing at room temperature in the Department of Human Anatomy of the School of Medicine of the University of Granada (Spain) between October and December 2020. Baseline SLIL integrity was confirmed in all wrists upon their dissection.

Experimental procedures

Scapholunate instability model. The model published by Pollock et al. [25] and Lee et al. [26] was followed but without using an arthroscope. The *extensor retinaculum* was accessed by dorsal approach and divided between third and fourth compartments. After radial separation of the tendon of the *extensor pollicis longus* (EPL) and ulnar separation of the tendons of the *extensor digitorum comunis* and *extensor index propius*, a dorsal capsulotomy was performed, sacrificing the dorsal intercarpal and dorsal radiocarpal ligaments (secondary dorsal capsuloligamentous stabilizers). After exposing the proximal row of the carpus, the SLIL was sectioned with a scalpel into dorsal, membranous, and volar components, confirming that the isolated sectioning of this ligament was insufficient to cause static scapholunate instability. When previous SLIL damage was observed during the dissection (n=2), the specimen was excluded from the study. The tendon of the *flexor carpi radialis* (FCR) was then ulnarly displaced by volar approach to expose and section the long radioscaphocapitate and

scaphotrapeziotrapezoid ligament complex (volar secondary stabilizers), observing the emergence of scaphoid rotatory subluxation.

One or more metal markers (heads of screws) of 4 mm diameter were inserted into the radius and carpal bones for the scaling of radiographic measurements. Radiographs in AP view in which the marker was perfectly circular and linear in lateral view were selected.

Before performing the instability model, tendons of the extensor carpi radialis longus (ECRL), extensor carpi radialis brevis (ECRB), and extensor carpi ulnaris (ECU) proximal to the extensor retinaculum were localized and labeled with 2-0 Vicryl suture in a dorsal approach. Tendons of the FCR and flexor carpi ulnaris (FCU) were identified in the same manner in a palmar approach. Specimens were stabilized on a radiotransparent table in horizontal position, and each labeled tendon was sequentially subjected to a load of 5 Lb measured by a digital dynamometer for the radiographic views in traction detailed below (Fig. 1). The order of sequential traction of the tendons was: ECRL and ECRB, ECU, FCU, and FCR.

Distal radius flexion osteotomy

The same dorsal approach was used to extraperiostally expose the distal metaphysis of the radius. Next, dorsal opening wedge osteotomy was performed with 20º flexion from the original position of the distal joint surface of the radius, immediately proximal to the distal radioulnar joint, using a 10-mm oscillating saw and osteoclasis of the palmar cortex, followed by fixation with a screwed dorsal 5-hole plate

Radiographic evaluation

All procedures and measurements were performed on a radiotransparent hand table (Fig. 1) in the experimental operating room under biosafety conditions. The hand was held in a device whose screws passed through the ulna and radius (after drilling), preventing any variations in the position of the specimen or in the pronosupination of the forearm and thereby guaranteeing the reproducibility of measurements. Biplanar radioscopy with a C-arm fluoroscope (PHILIPS BV25) was used for carpal kinematic evaluation before and after the instability model and after the radius flexion osteotomy. Radiographic images were captured in anteroposterior (AP) and lateral (L) views according to the following sequence: 1. AP view with no tendon traction in neutral alignment: maximum ulnar deviation and maximum radial deviation; 2. AP view in traction of ECRB and ECRL, ECU tendon, FCU tendon, and FCR tendon, successively; 3. L view without tendon traction in neutral, maximum extension, and maximum flexion; and 4. L view with FCR traction.

Instrument, measures, and variables

Images obtained in AP view were used to measure the apparent length (in mm) of the carpal scaphoid as indicator of scaphoid flexion and scapholunate interval, scaled using the metal radiographic markers.

Images in L view were used to determine the scapholunate angle, radiolunate, and palmar tilt of the distal joint surface of the radius in hexadecimal

degrees and to measure the dorsal scaphoid translation (DST) by the concentric circles method [27]. Briefly, contours of the proximal scaphoid pole and scaphoid facet of the distal radius were outlined using an electronic circle template on the radiographic image (Fig. 2). The DST was determined as the distance between the centers of these circles parallel to the long axis of the radius.

Radiographic measurements were performed by two independent observers using Angle Meter 360 software version 19 developed by Alexey Kozlov, considering the mean results in analyses.

Statistical analysis

SPSS v.25.0. (IBM Corp., Armonk NY) was used for statistical analyses. Results were expressed as means ± standard deviation. The Wilcoxon test was applied to compare results before and after the instability model and after the experimental treatment. An α error of 5% was accepted with 95% confidence interval, considering $p<0.05\%$ to be significant.

RESULTS

Tables 1-4 exhibit the radio-kinematic values obtained and the statistical significance of comparisons.

Radio-kinematic behavior of the carpus after performing the instability model

Isolated SLIL sectioning produced only subtle visual changes in scaphoid alignment. Evident flexion was solely observed after the additional sectioning of secondary scapholunate stabilizers, especially the scaphotrapeziotrapezoid ligament.

The radioscopic study in AP view (Table 1) confirmed that the whole proximal row of the carpus was extended in maximum passive ulnar deviation and in traction of the ECU tendon, with maximum scaphoid length and increased scapholunate interval. In contrast, the proximal row of the carpus was flexed in maximum passive radial deviation, observing emergence of the ring sign. Scaphoid flexion further increased with respect to passive radial deviation in FCR traction, when radioscopy showed a decrease in scaphoid length, increase in scapholunate interval, and dorsoradial subluxation of the scaphoid on the radius. FCU traction also induced scaphoid flexion, although this was less marked and there was a smaller increase in scapholunate interval. ECRB and ECRL traction reversed the misalignment, producing scaphoid extension, ring sign correction, and scapholunate interval reduction.

As observed in Table 2, the scapholunate gap was significantly increased in the instability model in all AP views except in radial deviation and in traction of ECRB and ECRL. However, no significant differences in scaphoid length were found between baseline (step A) and post-ligament sectioning (step B).

In L views, the scapholunate angle was always increased after performing the instability model (Table 3), observing the highest scapholunate angles with wrist flexion and FCR traction (87.81º$\pm$15.94 and 81.80º$\pm$12.14, respectively) and the highest DST values (3.81$\pm$1.39 mm) with FCR traction.

The scapholunate angle significantly increased in all L views between baseline and the instability model; however, the increase in DST was only significant with FCR traction (Table 4).

Radio-kinematic behavior of the carpus after distal radius flexion osteotomy

Scapholunate congruence was improved after osteotomy (Fig. 3), when the radioscopic study showed correction of static misalignment in AP (Fig. 4) and L views in neutral (Fig. 5) and correction of dorsal scaphoid subluxation in FCR tendon traction (Fig. 6).

The scapholunate interval significantly decreased after osteotomy in all static AP views and in tendon traction (Tables 1 and 2).

In L views, the palmar tilt increased by an average of 15-20º as determined by flexion osteotomy. The scapholunate angle was significantly decreased in all views and the DST was decreased in static L view in extension and in FCR traction, which demonstrated the greatest effect on dorsal scaphoid subluxation (Tables 3 and 4).

Radio-kinematic differences in the carpus between baseline and after distal radius flexion osteotomy

Flexion osteotomy appeared to restore specimens to a very similar carpal alignment to that observed at baseline, and this observation was confirmed by comparison of radiographic measurements, except for the inevitable increase in

palmar tilt. No significant differences were observed between baseline and post-osteotomy in the scapholunate interval (Table 2), the scapholunate angle in any L view, or the DST in FCR traction (Table 4).

DISCUSSION

Scapholunate instability is a frequent health problem, although its true prevalence is unknown [28]. Its maximum incidence is reached during the third and fourth decade of life, impairing the work and sports activities in which individuals of this age tend to be fully engaged [29]. In particular, scapholunate instability is one of the commonest causes of wrist osteoarthritis [9,17]. Numerous surgical procedures have been published for the treatment of these patients, but the optimal approach has yet to be established.

Naqui et al. [30] published a systematic review in 2018 on the management of chronic scapholunate dissociation. They included 17 out of a total of 1191 retrieved studies, identifying 27 different surgical techniques published before 2015 for the treatment of some stage of scapholunate instability. All selected studies offered level IV evidence, describing a 54% reduction in pain, 24% increase in grip strength, and 18% loss of flexion arc. Some type of complication was reported in 20% of patients, and there was also a relatively high rate (3.8%) of complex regional pain syndrome (CRPS). Complications and reconstruction failures led to revision surgery in 15% of cases. According to the authors of this review, there was insufficient evidence to recommend any treatment of chronic SLIL lesion over any other.

We propose a treatment line that completely differs from previously published approaches, acting on the orientation of the articular facet of the radius to contain DST. We describe the first experimental study of distal radius osteotomy for scapholunate instability, which obtained encouraging results.

The cadaveric instability model selected is widely endorsed in the literature [25,26,31], and recent studies have continued to perform biplane, static, and dynamic radiographic evaluations of models [32]. However, the clenched fist stress view described in other studies [33,34] was replaced with the stress view in FCR traction to reveal greater misalignments in the carpus.

The bony anatomy of the radius and scaphoid plays a role in stabilizing the carpus after ligament injury. In a cadaveric model of substitution of the proximal pole of the scaphoid to treat proximal pole nonunions, Capito and Higgins [35] observed that the preservation or reconstruction of scapholunate integrity may not be necessary if the reconstruction expands the normal dimensions of the native scaphoid. Scapholunate interval and carpal alignment may be restored by scaphoid overstuffing, as confirmed in a cadaveric model of scapholunate instability by Furey et al. [36], who concluded that scaphoid lengthening may represent a future direction for the surgical treatment of scapholunate instability.

In a study of eight cadaver specimens with sectioned scapholunate stabilizing ligaments, Werner et al. [37] used a wrist movement simulator to evaluate stability and observed that radioscaphoid fossa and scaphoid curvatures were larger in the wrists that did not evidence gross instability. Greater stability was also recorded in wrists with deeper radioscaphoid fossa and higher volar tilt.

Omori et al. [15] studied six patients with stage IV scapholunate dissociation and dorsal intercalated segment instability deformity, three of whom had a dorsally displaced distal radius malunion. The authors created three-dimensional bone models of the wrists from CT scans and calculated the centroid locations of each carpal bone and the rotational angle of the scaphoid and lunate relative to the radius, comparing the results with normal subjects. They demonstrated that pathological dorsal inclination of the distal surface of the radius intensified the joint alterations described in scapholunate instability, reducing the contact area and increasing the pressure on radio-scaphoid, midcarpal, and scaphotrapeziotrapezoid joints. These findings prompted our team to hypothesize that radiocarpal and midcarpal joint congruence could be improved in patients with scapholunate instability by a modification in the opposite direction, changing the flexion of the joint surface of the radius.

In brief, the aim of flexion osteotomy is to modify the radioscaphoid relationship so that the dorsal ridge of the radius constrains DST, a traditional approach to joint instability in the shoulder and elsewhere [38]. The present results demonstrate a significant reduction in DST after osteotomy, especially in FCR traction, the most destabilizing dynamic radiographic examination.

Flexion osteotomy can be performed with an addition (“open wedge”) or subtraction (“closed wedge”) effect, and the former was arbitrarily selected for this study. This involves a relative lengthening of the radius, producing a situation analogous to that described by Capito and Higgins [35] and Furey et al. [36], in which the scapholunate interval and carpal alignment were restored by scaphoid overstuffing. It would be of interest to repeat the experiment with a subtraction

(shortening) osteotomy in order to compare the effects and identify the critical flexion angle in the osteotomy.

Injury to the scapholunate ligament alone does not cause scapholunate instability, and secondary stabilizing ligaments must also be impaired to produce scapholunate diastasis, flexion, and pronation of the scaphoid [4]. As noted by Furey, et al [36], isolated SLIL reconstruction affects only one aspect of instability and is likely insufficient to reestablish normal carpal biomechanics.

Lengthening of the scaphoid or radius would produce a retightening of radiocarpal capsule and secondary stabilizers. This may restore carpal alignment without SLIL reconstruction, as observed in the present experiment, correcting the scapholunate interval, scapholunate and radioulnar angles, and DST.

One concern arising from this experiment, as also observed in scaphoid lengthening studies [35,36], is the potential increase in contact pressures between scaphoid and radius articular surfaces. The repercussions of this increase on wrist mobility and progression to wrist osteoarthritis must be considered before this technique is applied in patients.

One limitation of this cadaveric study is that it was based on a small number of specimens and did not allow examination of the clinical repercussions and joint kinematics under neuromuscular control *in vivo*. It was also not possible to evaluate the impact of modifying joint load transmissions or the effects of osteotomy on functional arcs of wrist motion after osteotomy. In addition, only AP and L radiological views were used for measurements, yielding information in 2D that could be completed by 3D evaluation and with a CT scan. Furthermore, the generic fixation material employed for osteotomy stabilization is very different

from radius-specific fixation systems of anatomical design. Finally, although these results are encouraging, a prospective *in vivo study* with control group is needed to determine the mid- and long-term outcomes of these procedures, because these findings reflect only the immediate post-surgical condition, which may possibly deteriorate with repetitive motion and the stretching of soft tissues.

In conclusion, distal radius flexion-addition osteotomy appears to improve carpal alignment parameters (scapholunate interval, scapholunate angle, and DST) in a cadaveric model of static scapholunate instability, reaching similar values to those observed pre-instability at baseline. However, its application in the clinical setting is yet to be demonstrated.

REFERENCES

1. Andersson JK. Treatment of scapholunate ligament injury: Current concepts. EFORT Open Rev. 2017;2(9):382-393.
2. Johnson JE, Lee P, McIff TE, Toby EB, Fischer KJ. Scapholunate ligament injury adversely alters in vivo wrist joint mechanics: an MRI-based modeling study. J Orthop Res. 2013, 31: 1455–60.
3. Short WH, Werner FW, Green JK, Masaoka S. Biomechanical evaluation of ligamentous stabilizers of the scaphoid and lunate. J Hand Surg Am. 2002; 27(6):991-1002.
4. Short WH, Werner FW, Green JK, Masaoka S. Biomechanical evaluation of the ligamentous stabilizers of the scaphoid and lunate: Part II. J Hand Surg Am 2005;30(01):24–34

5. Short WH, Werner FW, Green JK, Sutton LG, Brutus JP. Biomechanical evaluation of the ligamentous stabilizers of the scaphoid and lunate: part III. J Hand Surg Am. 2007;32(3):297-309.
6. Kitay A, Wolfe SW. Scapholunate instability: current concepts in diagnosis and management. J Hand Surg Am. 2012;37(10):2175-2196.
7. Werner FW, Short WH, Green JK. Changes in patterns of scaphoid and lunate motion during functional arcs of wrist motion induced by ligament division. J Hand Surg Am. 2005; 30:1156–60.
8. Pappou IP, Basel J, Deal DN. Scapholunate ligament injuries: a review of current concepts. Hand (N Y). 2013;8(2):146-156.
9. Watson HK, Weinzweig J, Zeppieri J. The natural progression of scaphoid instability. Hand Clin. 1997, 13: 39–49.
10. Messina JC, Van Overstraeten L, Luchetti R, Fairplay T, Mathoulin CL. The EWAS classification of scapholunate tears: an anatomical arthroscopic study. J Wrist Surg 2013;2(02):105–109
11. Dreant N, Mathoulin C, Lucchetti R, et al. Comparison of two arthroscopic classifications for scapholunate instability. Chir Main. 2009;28(2):74-7.
12. Geissler W B, Haley T. Arthroscopic management of scapholunate instability. Atlas Hand Clin. 2001; 6:253–274.
13. Garcia-Elias M, Lluch AL, Stanley JK. Three-ligament tenodesis for the treatment of scapholunate dissociation: indications and surgical technique. J Hand Surg Am. 2006;31(1):125–134.
14. Short WH, Werner FW, Fortino MD, Palmer AK, Mann KA. A dynamic biomechanical study of scapholunate ligament sectioning. J Hand Surg Am. 1995, 20: 986–99.
15. Omori S, Moritomo H, Omokawa S, Murase T, Sugamoto K, Yoshikawa H. In vivo 3-dimensional analysis of dorsal intercalated segment instability deformity secondary to scapholunate dissociation: a preliminary report. J Hand Surg Am. 2013;38(7):1346-1355.

16. Blevens AD, Light TR, Jablonsky WS, Smith DG, Patwardhan AG, Guay ME, Woo TS. Radiocarpal articular contact characteristics with scaphoid instability. J Hand Surg Am. 1989;14(5):781-90.
17. Watson HK, Ballet FL. The SLAC wrist: scapholunate advanced collapse pattern of degenerative arthritis. J Hand Surg 1984;9A:358–365.
18. Montgomery SJ, Rollick NJ, Kubik JF, Meldrum AR, White NJ. Surgical outcomes of chronic isolated scapholunate interosseous ligament injuries: a systematic review of 805 wrists. Can J Surg. 2019;62(3):1-12.
19. Imada AO, Eldredge J, Wells L, Moneim MS. Review of surgical treatment for chronic scapholunate ligament reconstruction: a long-term study. Eur J Orthop Surg Traumatol. 2022 May 24.
20. Daly LT, Daly MC, Mohamadi A, Chen N. Chronic Scapholunate Interosseous Ligament Disruption: A Systematic Review and Meta-Analysis of Surgical Treatments. Hand (N Y). 2020; 15(1):27-34
21. Szabo RM, Slater RR Jr, Palumbo CF, Gerlach T. Dorsal intercarpal ligament capsulodesis for chronic, static scapholunate dissociation: clinical results. J Hand Surg Am 2002;27(06):978–984
22. Moran SL, Ford KS, Wulf CA, Cooney WP. Outcomes of dorsal capsulodesis and tenodesis for treatment of scapholunate instability. J Hand Surg Am 2006;31(09):1438–1446.
23. De Smet L, Goeminne S, Degreef I. Failures of the three-ligament tenodesis for chronic static scapholunate dissociation are due to insufficient reduction. Acta Orthop Belg. 2011; 77(5):595-7.
24. Goeminne S, Borgers A, van Beek N, De Smet L, Degreef I. Long-term follow-up of the three-ligament tenodesis for scapholunate ligament lesions: 9-year results. Hand Surg Rehabil. 2021; 40(4):448-452.
25. Pollock PJ, Sieg RN, Baechler MF, Scher D, Zimmerman NB, Dubin NH. Radiographic evaluation of the modified Brunelli technique versus the Blatt

capsulodesis for scapholunate dissociation in a cadaver model. J Hand Surg Am. 2010;35(10):1589-98.

26. Lee SK, Desai H, Silver B, Dhaliwal G, Paksima N. Comparison of radiographic stress views for scapholunate dynamic instability in a cadaver model. J Hand Surg Am. 2011 Jul;36(7):1149-57.
27. Chan K, Vutescu ES, Wolfe SW, Lee SK. Radiographs Detect Dorsal Scaphoid Translation in Scapholunate Dissociation. J Wrist Surg. 2019; 8(3):186-191.
28. O'Brien L, Robinson L, Lim E, O'Sullivan H, Kavnoudias H. Cumulative incidence of carpal instability 12-24 months after fall onto outstretched hand. J Hand Ther. 2018;31(3):282-286.
29. Melsom D, Leslie I. Carpal dislocations. Curr Orthop. 2007; 21:288e297.
30. Naqui Z, Khor WS, Mishra A, Lees V, Muir L. The management of chronic non-arthritic scapholunate dissociation: a systematic review. J Hand Surg Eur Vol. 2018; 43(4):394-401.
31. Payet E, Bourguignon D, Auquit-Auckbur I, Duparc F, Dujardin F. Radiographic evaluation of a novel horizontal dorsal intercarpal capsulodesis as a treatment of pre-arthritic scapholunate dissociation: a cadaver study. J Hand Surg Eur Vol. 2015; 40(5):502-11.
32. Burnier M, Jethanandani R, Pérez A, Meyers K, Lee S, Wolfe SW. Comparative Analysis of 3 Techniques of Scapholunate Reconstruction for Dorsal Intercalated Segment Instability. J Hand Surg Am. 2021; 46(11):980-988.
33. Hsu JW, Kollitz KM, Jegapragasan M, Huang JI. Radiographic evaluation of the modified Brunelli technique versus a scapholunotriquetral transosseous tenodesis technique for scapholunate dissociation. J Hand Surg Am. 2014; 39(6):1041-9.
34. Athlani L, Pauchard N, Dautel G. Radiological evaluation of scapholunate intercarpal ligamentoplasty for chronic scapholunate dissociation in cadavers. J Hand Surg Eur Vol. 2018; 43(4):387-393.

35. Capito AE, Higgins JP. Scaphoid overstuffing: the effects of the dimensions of scaphoid reconstruction on scapholunate alignment. J Hand Surg Am. 2013;38(12):2419-2425.
36. Furey MJ, White NJ, Dhaliwal GS. Scapholunate Ligament Injury and the Effect of Scaphoid Lengthening. J Wrist Surg. 2020; 9(1):76-80.
37. Werner FW, Short WH, Green JK, Evans PJ, Walker JA. Severity of scapholunate instability is related to joint anatomy and congruency. J Hand Surg Am. 2007 Jan;32(1):55-60.
38. Latarjet M. Treatment of recurrent dislocation of the shoulder. Lyon Chir 1954; 49:994–997.

FIGURES

Fig. 1

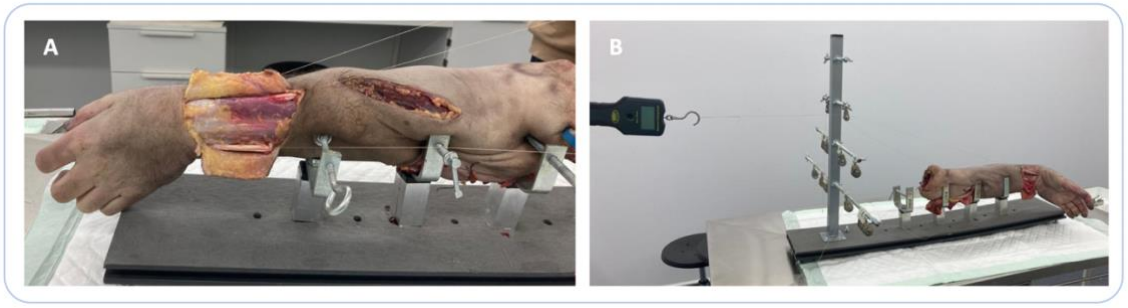

A: Radiolucent specimen fixation device with pulleys for tendon traction. **B:** Traction force controlled with digital dynamometer

Fig. 2

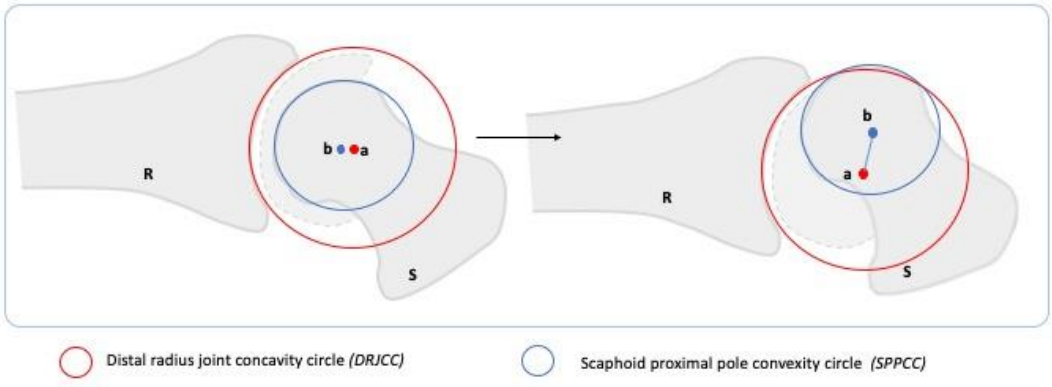

Dorsal scaphoid translation *(DST)* measurement published by Chan (2019); **a:** center of DRJCC; **b:** center of SPPCC; **ab** distance: DST; **R:** Radius; **S:** Scaphoid

Fig. 3

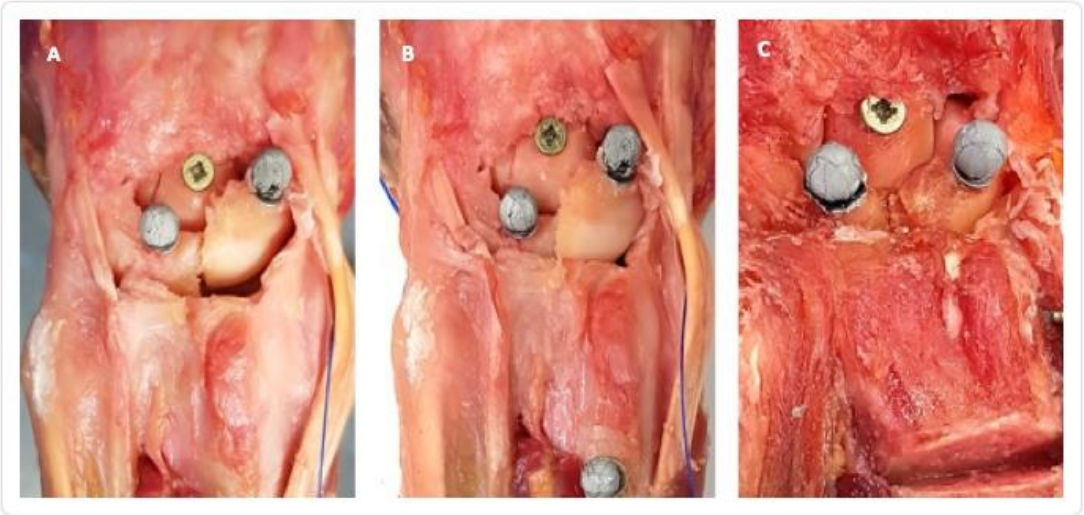

Effect of distal radius flexion osteotomy on carpus alignment. **A:** isolated scapholunate ligament (SLIL) injury. **B:** Complete scapholunate instability model (division of SLIL + secondary stabilizers). **C:** Effect of distal radius flexion osteotomy on scapholunate joint

Fig. 4

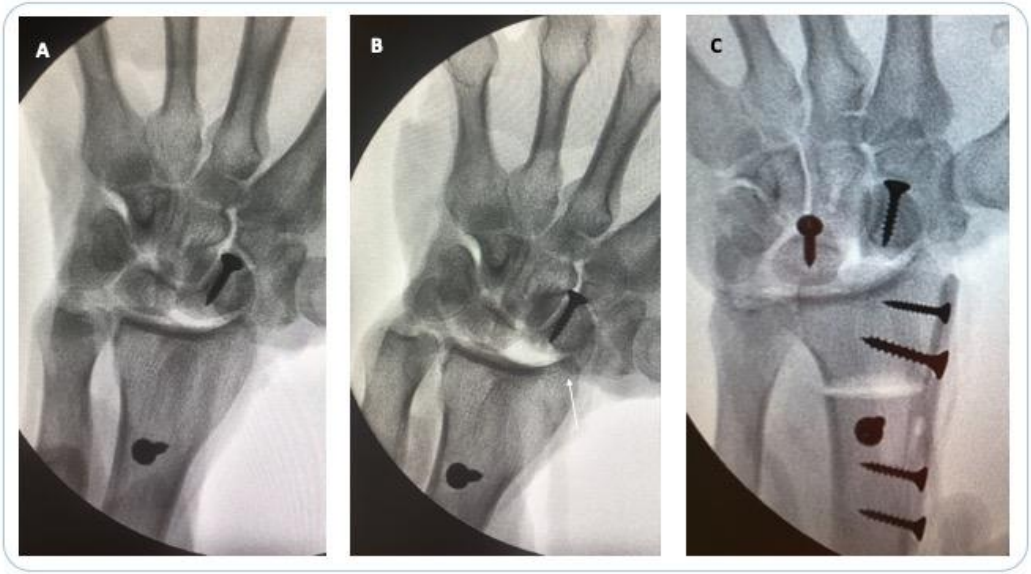

Radiographical behavior of the carpus in Anteroposterior view in Flexor Carpi Radialis tendon traction. **A:** Baseline **B:** Instability model completed. The superimposition of the contour of the scaphoid on the radius is observed as an indirect sign of radioscaphoid dislocation (white arrow). **C:** After distal radius flexion osteotomy. The ring sign is evident, but no radioscaphoid dislocation can be seen

Fig. 5

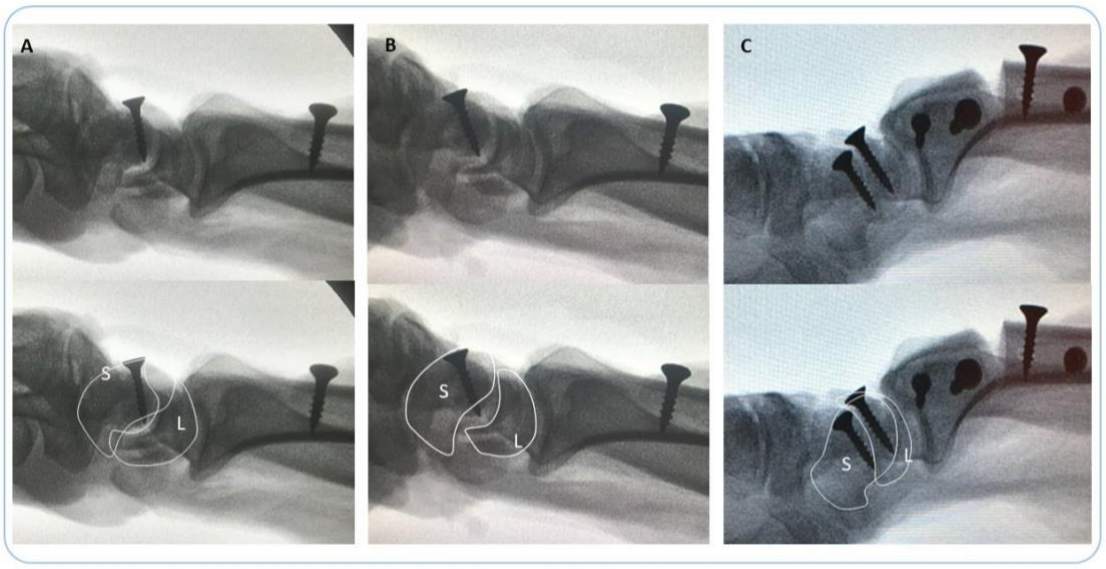

Radiographical behavior of the carpus in Lateral view: **A:** Baseline **B:** Instability model completed. Incongruity and increase in the scapholunate angle can be observed. **C:** After distal radius flexion osteotomy. The scaphoid subluxation is corrected. Scaphoid and lunate have returned to a normal relationship, and the scapholunate angle is normalized. *S:* Scaphoid. *L:* Lunate

Fig. 6

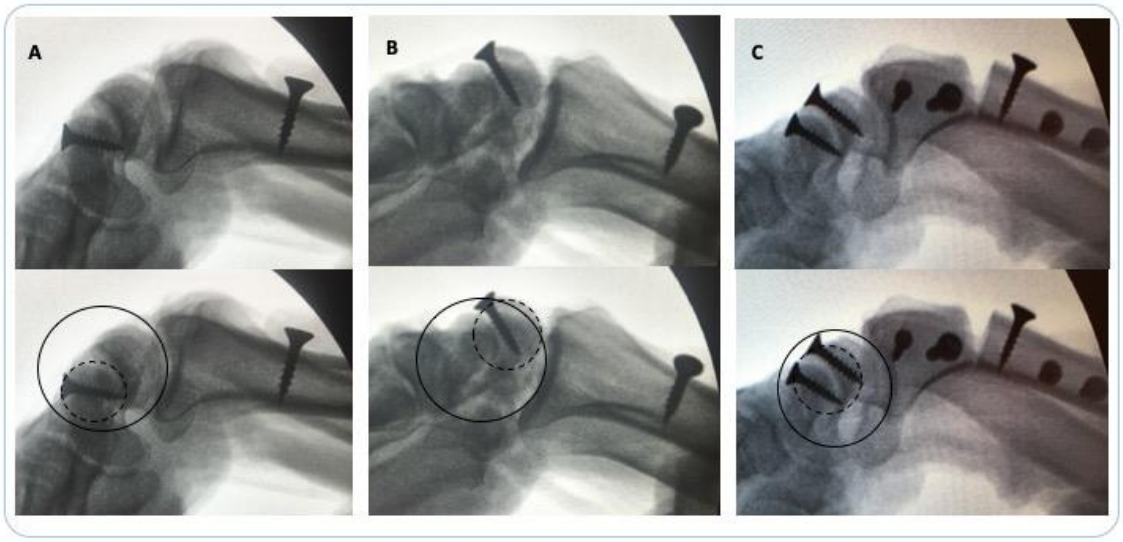

Radiographical behavior of the carpus in Lateral view in Flexor Carpi Radialis tendon traction. **A:** Baseline **B:** Instability model completed. Radioscaphoid subluxation can be observed. **C:** After distal radius flexion osteotomy. The scaphoid subluxation is corrected. Continuous line circle indicates the concavity of the radius joint surface, and the dotted line circle represents the scaphoid proximal pole to estimate the dorsal scaphoid translation

TABLES

TABLE 1

STEP	Variable	APN	APR	APU	APECR	APECU	APFCU	APFCR
A	Scaphoid length	20.47±3.02	21.17±5.58	27.92±4.18	22.80±3.49	26.06±5.11	20.94±4.65	15.82±2.32
	Scapholunate interval	1.76±0.46	1.88± 0.41	1.86±1	1.79 ± 0.67	2.25 ± 0.71	1.96 ±0.68	1.19±0.92
B	Scaphoid length	20.71±2.76	18.72±4.42	27.33±3.55	21.87±4.58	27.22±6.78	21.08±3.81	15.55±3.98
	Scapholunate interval	2.36±1.64	2.75±1.48	3.23±1.25	2.52±1.3	3.49±2.48	2.77±0.81	4.02±2.62
C	Scaphoid length	23.77±3.96	21.56±3.72	27.22±3.21	21.91±4.73	25.19±1.76	20.92±3.88	14.32±2.28
	Scapholunate interval	1.35±0.62	1.08±0.55	1.72±0.85	1.35±1.06	1.5±0.59	1.86±0.55	1.29±0.87

Table 1. Measurements (mm) means ± standard deviation in anteroposterior (AP) view. APN: AP view in neutral wrist position; APR: AP view in radial deviation; APU: AP view in ulnar deviation; APECR: AP view in *Extensor Carpi Radialis* tendon traction; APECU: AP view in *Extensor Carpi Ulnaris* tendon traction; APFCU: AP view in *Flexor Carpi Ulnaris* tendon traction; APFCR: AP view in *Flexor Carpi Radialis* tendon traction; A: Baseline. B: Instability model step; C: Flexion Osteotomy step

TABLE 2

	Variable	APN	APR	APU	APECR	APECU	APFCU	APFCR
A vs B	**Scaphoid length**	0.553	0.310	0.028	0.917	0.917	0.279	0.449
	Scapholunate interval	0.173	0.125	0.043	0.528	0.066	0.026	0.063
B vs C	**Scaphoid length**	0.055	0.131	0.937	0.755	0.594	0.754	0.154
	Scapholunate interval	0.024	0.004	0.003	0.003	0.005	0.004	0.04
A vs C	**Scaphoid length**	0.042	0.735	0.611	0.600	0.917	0.612	0.553
	Scapholunate interval	0.680	0.058	0.309	0.167	0.138	0.197	0.248

Table 2. P value by Wilcoxon test for differences in scaphoid length and scapholunate interval in anteroposterior (AP) view between baseline situation and instability model (AvsB), between instability model and after flexion osteotomy (BvsC), and between baseline and flexion osteotomy. APN: AP view in neutral wrist position; APR: AP view in radial deviation; APU: AP view in ulnar deviation; APECR: AP view in *Extensor Carpi Radialis* tendon traction; APECU: AP view in *Extensor Carpi Ulnaris* tendon traction; APFCU: AP view in *Flexor Carpi Ulnaris* tendon traction; APFCR: AP view in *Flexor Carpi Radialis* tendon traction; A: Baseline; B: Instability model step; C: Flexion Osteotomy step. Shaded box = statistically significant difference.

TABLE 3

STEP	Variable	LN	LE	LF	LFCR
A	Palmar tilt	9.95±3.92	13.15±4.45	13.92±3.22	17.72±6.63
	Scapholunate angle	58.47±7.96	42.48±17.47	59.35±12.37	63.40±20.66
	Radiolunate angle	15.22±9.01	26.44±10.01	19.85±8.98	21.46±5.54
	DST (mm)	2.38±1.36	1.98±2.45	2.21±1.94	1.55±1.15
B	Palmar tilt	14.18±5.85	14.85±4.63	15.65±7.33	15.16±4.54
	Scapholunate angle	71.70±10.73	56.82±19.63	87.81±15.94	81.80±12.14
	Radiolunate angle	23.69±18	31.3±7.82	26.82±6.47	26.85±11.11
	DST (mm)	2.11±2.35	3.24±2.53	2.37±2.55	3.81±1.39
C	Palmar tilt	29.75±5.18	28.14±9.41	32.19±7.21	34.64±8.59
	Scapholunate angle	50.75±14.54	33.15±12.45	59.71±11.41	68.73±19.65
	Radiolunate angle	11.91±9.39	15.73±9.89	30.73±18.69	24.80±13.49
	DST (mm)	0.45±0.94	0.49±0.83	1.24±2.07	0.38±0.59

Table 3. Mean measurements (mm and hexadesimal degrees) with standard deviations in lateral (L) view. LN: L view in neutral wrist position; LE: L view in extension; LF: L view in flexion; LFCR: L view in *Flexor Carpi Radialis* tendon traction; A: Baseline; B: Instability model step; C: Flexion Osteotomy step; Dorsal Scaphoid Translation (DST)

TABLE 4

	Variable	LN	LE	LF	LFCR
A vs B	Palmar tilt	0.063	0.463	[1]	0.225
	Scapholunate angle	0.018	0.018	0.018	0.018
	Radiolunate angle	0.091	0.398	0.046	0.225
	DST (mm)	0.465	0.463	0.893	0.028
B vs C	Palmar tilt	0.008	0.008	0.008	0.008
	Scapholunate angle	0.008	0.011	0.008	0.038
	Radiolunate angle	0.012	0.008	0.110	0.314
	DST (mm)	0.144	0.028	0.249	0.018
A vs C	Palmar tilt	0.018	0.028	0.018	0.043
	Scapholunate angle	0.735	0.051	[1]	0.893
	Radiolunate angle	0.091	0.018	0.735	0.686
	DST (mm)	0.08	0.345	0.600	0.144

Table 4. P value by Wilcoxon test for differences in palmar tilt, scapholunate angle, radiolunate angle, and dorsal scaphoid translation (DST) in lateral (L) view between baseline and instability model (AvsB), between instability model and after flexion osteotomy (BvsC), and between baseline and flexion osteotomy. LN: L view in neutral wrist position; LE: L view in extension; LF: L view in flexion; LFCR: L view in *Flexor Carpi Radialis* tendon traction; A: Baseline; B: Instability model step; C: Flexion Osteotomy step; Dorsal Scaphoid Translation (DST). Shaded box = statistically significant difference.